STRUCTURAL ORGANISATION OF THE WOOD POLYMERS IN THE WOOD FIBRE STRUCTURE

Lennart Salmén,[a,*] Anne-Mari Olsson,[a] Jasna S. Stevanic,[a] Jasna Simonović,[b] and Ksenija Radotić [b]

The organization of the major polymers in the wood fiber has a large impact on the properties of the structure. Numerous studies have been devoted to the cellulose microfibril arrangement, providing the longitudinal strength of the fiber, while less is known regarding the structural organization of other components, such as hemicelluloses and lignin. For the hemicelluloses, as being part of the cellulose aggregation process, indications of a strong coupling to the cellulose structure have been shown. For lignin, being laid down in a later stage, no clear picture has emerged. Here the orientation of lignin vis-à-vis the cellulose orientation was examined for a number of different fiber structures. It was shown that the lignin in the middle lamella region seems to be non-oriented, thus more resembling an isotropic material, while the lignin in the secondary wall is to some extent oriented. The orientation of this lignin is less pronounced than the orientation of cellulose but has a preferential alignment in the direction of the fiber axis. The reason for this alignment could be related to structural restrictions of this lignin, deposited in the spaces remaining after the initial forming of the structured cellulose/hemicellulose fibrillar structure.

Keywords: Cellulose; Lignin; Middle lamella; Orientation; Wood fibers

*Contact information: a: Innventia, Box 5604, SE-11486 Stockholm, Sweden; b: Institute for Multidisciplinary Research, Kneza Višeslava 1, Belgrade, 11000, Serbia; * Corresponding author: lennart.salmen@innventia.com*

INTRODUCTION

The structural organization of the wood polymers within the cell wall is highly complex and still awaiting its detailed description on the ultra-structural level. The organization and properties of the wood polymers to a large extent determines the properties of fibers and wood, and an understanding of the interaction between these polymers is a key to the genetic development of improved wood and fiber quality (Salmén 2004).

An important aspect of the wood polymer organization is the orientation of the different wood polymers within the major cell wall, the S_2 wall, of the fibers. The majority of studies regarding orientation have only focused on the cellulose microfibril orientation, which dominates how the mechanical properties in the fiber direction are perceived. However, the organization of the remaining wood polymers to a large extent influences transverse properties (Bergander and Salmén 2002). This organization is also of importance when understanding the cell wall formation during growth. During the process of cell wall formation the hemicelluloses are deposited simultaneously with the

organization of the cellulose microfibrils (Atalla et al. 1993; Terashima et al. 2009). Thus a high degree of association and orientation of the hemicellulose polymer in parallel to the cellulose microfibrils have been shown (Page 1976; Åkerholm and Salmén 2001; Stevanic and Salmén 2009). For the lignin, having been laid down later in spaces remaining, it may be anticipated that structural restrictions may impose or restrict its organization (Terashima 1990; Jurasek 1998). Indeed, Atalla and Agarwel (1985) have demonstrated that the lignin aromatic ring shows an orientation parallel to the cell wall surface, i.e. in the tangential direction of the fiber wall. However, so far the picture seems not clear with regard to any lignin orientation parallel to the fiber axis, with some data supporting orientation while others do not show such a clear case (Åkerholm and Salmén 2003; Stevanic and Salmén 2009; Olsson et al. 2011; Simonović et al. 2011). Thus, in order to shed some more light on this question, a more in depth analyses of lignin orientation across the cell wall structure, including the middle lamella as well as the secondary wall, was performed using polarized imaging FTIR (iFTIR) microscopy. A comparison to measurements on different wood fiber structures was also made.

Polarized iFTIR microscopy has, in particular, been utilized for studies on different wood tissues for investigating the orientation of the wood polymers (Stevanic and Salmén 2009; Olsson et al. 2011). Measurements have been performed in transmission mode on microtome cut samples in the longitudinal-radial direction of the wood as well as on single wood fibers isolated by various means. Signals specific for the main components of cellulose, lignin, glucomannan and xylan were identified and used to monitor the orientation of the polymers in relation to the main axis of the fiber.

EXPERIMENTAL

Materials

Wood fiber materials from different species, both of softwood and hardwood, were used; softwood: Norwegian spruce (*Picea abies* (L.) Karst.) and Serbian spruce (*Picea omorika (Pančˇ) Purkyne*); hardwood; maple (*Acer sp*.) and hybrid aspen (*Populus tremula* x tremuloides). The preparation of the different species was not identical due to the fact that the samples initially were used for other studies; thus some samples were studied as microtome cuts while others were measured on isolated fibers. In order to assure a low microfibril angel, MFA, of these samples they were, if not otherwise specified, taken from mature wood avoiding any presence of reaction wood. A MFA of less than 20^{o} would thus be assumed for these samples (Sahlberg et al. 1997; Bergander et al. 2002).

Norwegian spruce

A radial microtome cut of 20 μm in thickness from the mature part of a 40 year old spruce was prepared in order to have a section with pure middle lamella regions together with double cell wall regions. For comparison, single fibers taken from the first stage of a TMP (thermo mechanical pulp) production and treated mechanically in a disintegrator to remove the outer layers of the fiber walls, i.e. ML (middle lamella), P (primary wall) and S_1 (secondary wall; 1st layer) were used (Stevanic and Salmén 2009).

These 'native' fibers were thus mainly containing the S_2 and S_3 cell wall layers, as verified by microscopic images (Stevanic and Salmén 2009).

Serbian spruce

Fiber material was prepared by disintegration from the mature part of straight branches, free from compression wood (Simonović et al. 2011).

Maple

Fiber material was prepared by disintegration from the mature part of straight branches, free from tension wood (Simonović et al. 2011).

Hybrid aspen

Microtome sections (tangential x longitudinal) were made from the outer part of the stem of 1.5 m high hybrid aspen (*Populus tremula* x tremuloides; T89) trees grown in greenhouse (Olsson et al. 2011). The fibers had a MFA of 15° as determined by X-ray (Bjurhager et al. 2010).

Methods

FTIR microscopy measurements were carried out using a Spectrum Spotlight 400 FTIR Imaging System (Perkin Elmer Inc, Shelton, CT, USA). The area of interest was first displayed, using a CCD camera, to locate the cell wall area, which was then irradiated using mid-IR light. The scanning was carried out in imaging mode using an array detector, providing a pixel resolution of 6.25 μm x 6.25 μm (for the hybrid aspen only an average area of a resolution of 100 μm x 100 μm was examined), a spectral resolution of 4 cm^{-1}, and a spectral range from 4000 cm^{-1} to 720 cm^{-1}.

Two absorption peaks were specifically selected as markers for the polymers; for lignin the 1506 cm^{-1} characteristic of the aromatic ring (Faix 1991) and for cellulose the 1160 cm^{-1} as characteristic of the carbohydrate glucosidic bond and the glucose ring (Liang and Marchessault 1959). As absorbance peaks in FTIR are often overlapping the focus in this work has been on these two more or less non-interfering peaks (Gierlinger et al. 2008). The cellulose 1425 cm^{-1} peak, characteristic of the C-OH bending vibration of the CH_2-OH group absorbing in the direction along the chain was also chosen for comparison (Åkerholm et al. 2004).

The orientation of different absorption peaks were given based on the relative absorbance, *RA*, calculated as Eq. 1:

$$RA = (I_p - I_{min})//I_{max} - I_{min}) \quad (1)$$

where I_p is the intensity of the absorbed IR radiation at a given angle of polarization, I_{max} is the maximum intensity in the polarization interval (0°-90°), and I_{min} is the minimum intensity in the polarization interval (0°-90°). To further examine the orientation dependence of the polymers vector diagrams of the absolute absorbances were displayed.

RESULTS AND DISCUSSION

A number of different wood tissues were examined with regard to the orientation of lignin and of the carbohydrates, primarily the cellulose.

Norwegian Spruce

Figure 1 shows a light microscope picture of a radially cut earlywood section together with an FTIR image of the total absorbance, reflecting the material quantity, in different areas of this section. Fiber walls areas and middle lamella areas may here be distinguished. An FTIR spectra from a double cell wall area (6.25 μm^2) of this section is displayed in Fig. 2 together with the absorbance difference (0^o - 90^o) indicating the clear orientation signals at 1506 cm^{-1} (lignin) and 1160 cm^{-1} (cellulose). Although cellulose in the region of 950 to 1180 cm^{-1} displays several intense, sometimes overlapping bands (Wiley and Atalla 1987), it seems clear that in FTIR the C-O-C stretching at 1160 cm^{-1} is the dominant absorption band indicating orientation of the carbohydrates (Fig. 2), in similarity with the band at 1095 cm^{-1} in Raman spectroscopy (Wiley and Atalla 1987; Gierlinger et al. 2006). It has also been demonstrated that the 1160 cm^{-1} band displays the similar response to mechanical straining (Salmén and Bergström 2009) as the 1095 cm^{-1} band does in Raman spectroscopy (Gierlinger et al. 2006; Hsieh et al. 2008).

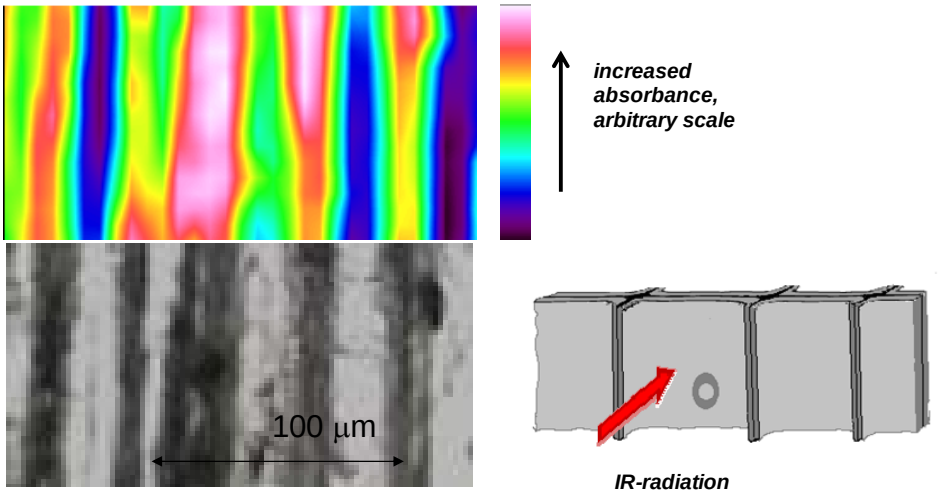

Fig. 1. Microscopic picture (bottom) of a radially cut cross section through the earlywood of an annual ring of spruce wood (schematically drawn to the right). Fibers are oriented top to bottom of the figure. The top figure displays the FTIR imaging picture of the total absorbance of the same region (absorbance between 4000 and 720 cm^{-1}). Higher total absorbance (more towards red color) indicates a higher amount of material, i.e. the position of the tangential cell walls.

In Fig. 3 the specific absorbance and the absorbance ratio (0^o/90^o) for lignin and cellulose across the wood section is shown. The specific absorbance is taken as the absorbance maximum for lignin (1506 cm^{-1}) and cellulose (1160 cm^{-1}) respectively, divided by the total absorbance between 1800 and 720 cm^{-1} for each pixel along a line scanning the cross section. Thus these values indicate the relative abundance of lignin and cellulose respectively, in each position across the section. The cellulose signals

showed a clear orientation with only exceptional points of no orientation (absorbance ratio close to 1). For lignin, the orientation degree was much lower with more frequent areas of no or very low degree of orientation.

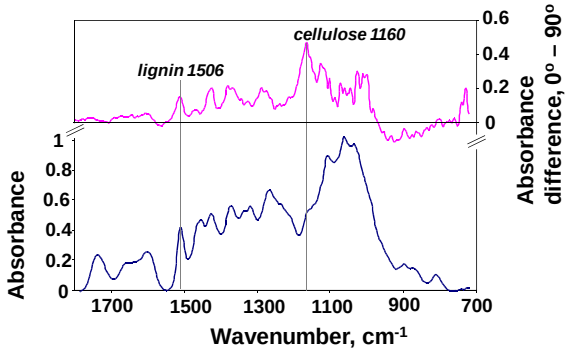

Fig. 2. Average absorbance from one typical radial double cell wall fiber area (6.25 x 6.25 μm) of the radial wood section (Fig. 1) as a function of wavenumber, cm^{-1}, as well as the average absorbance difference, 0^o - 90^o from spectra from this area.

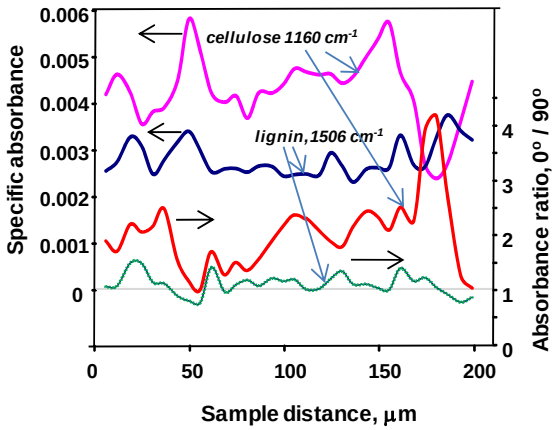

Fig. 3. Specific absorbance, related to the total absorbance between 1800 to 720 cm^{-1} in each point, and absorbance ratio (0^o/90^o) of lignin and cellulose across a radial section of spruce wood.

Figure 4 shows the relative absorbance for lignin and cellulose from an area of the double cell wall, here as a function of the polarization angle. It is obvious that the cellulose showed a strong indication of an orientation of the microfibrils at an angle close to zero, i.e. corresponding to the longitudinal fiber axis. For the lignin the orientation was less precise although a preference for an orientation of the phenylpropane units in the longitudinal direction of the fiber, i.e. in the direction of the cellulose microfibrils seems clear.

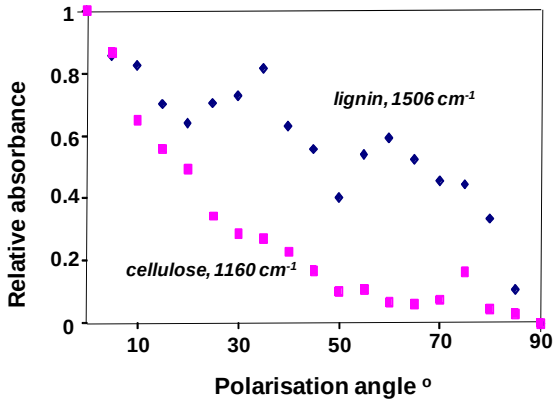

Fig. 4. Orientation distribution of absorbance for lignin and cellulose in a double cell wall area of spruce wood. Peak values for different polarizations were normalized to the interval from 0 to 1.

If instead observing the orientation dependence of the total absorption, as in Fig. 5, it is clear that, for both the lignin and cellulose peak, there was a large absorption not only at 0^o polarization but also at 90^o polarization. The cellulose shows a much higher degree of orientation than that of the lignin. A component of oriented lignin is however quite clear from the comparison with the orientation distribution for a fully isotropic

material, as represented by the dotted line. One must also here keep in mind that IR spectra often contain overlapping peaks, or peaks that are not fully resolved. Thus, the lignin absorption peak at 1506 cm^{-1} is to some extent influenced by the orthogonally oriented CH_2 vibration of xylan (Marchessault 1962) at 1460 cm^{-1}. The absorbance at this wavenumber is generally low at 0^o and high at 90^o (assumed to reflect an orientation of xylan along with the cellulose (Stevanic et al. 2009; Olsson et al. 2011)) thus counteracting the orientation signal seen for the lignin at 1506 cm^{-1}. For the cellulose, all peaks are heavily overlapping. To illustrate the relations, one may look at the cellulose C-OH bending vibration at 1425 cm^{-1} (Åkerholm et al. 2004), which shows a distinct peak at all polarization angles. In Fig. 6 the orientation dependence is compared for the total absorption (peak to baseline) of the 1425 cm^{-1} vibration with that of the 1425 cm^{-1} peak itself (taken from a line connecting the valleys on each side of the peak at 1445 cm^{-1} and 1400 cm^{-1}, respectively). Obviously, such an estimation of the contribution of the absorption at 1425 cm^{-1} is somewhat underestimating the actual contribution from the C-OH bending, as a large portion of the absorption signal is neglected (the difference between the signal of total absorption and peak absorption in Fig. 6), as some of this absorption must be attributed to the 1425 cm^{-1} vibration. From the behavior of the peak absorption in Fig. 6 it is though clear that a very distinct orientation of the cellulose microfibrils around 0^o to 5^o may be estimated, the angle of the maximal vector length.

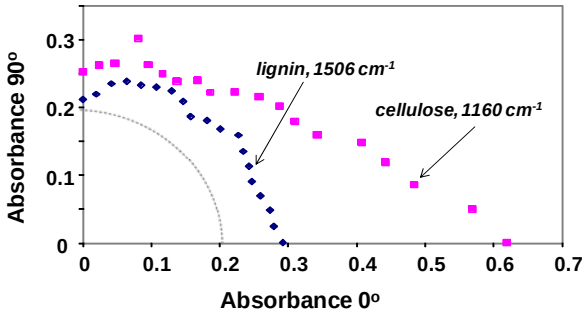

Fig. 5. Polar diagram (0^o to 90^o) of the absolute absorbance of lignin and cellulose for a double cell wall area of spruce wood. 0^o polarization is in the longitudinal fiber direction. Each data point represents a measurement between 0^o and 90^o polarization taken every 5^o. The dotted line represents non-oriented substances.

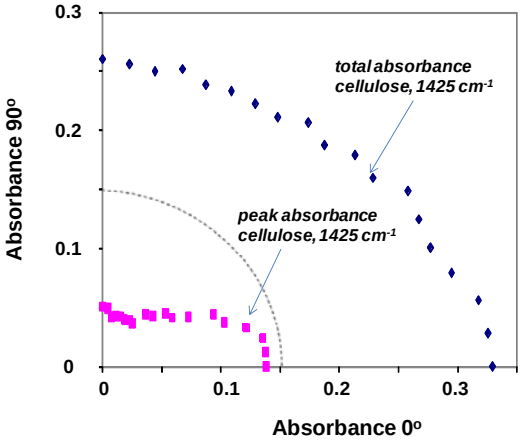

Fig. 6. Polar diagram (0^o to 90^o) of the absolute absorbance as well as the peak absorption for the cellulose C-OH bending peak at 1425 cm^{-1} for the secondary wall of a TMP fiber. 0^o polarization is in the longitudinal fiber direction. Each data point represents a measurement between 0^o and 90^o polarization taken every 5^o.The dotted line represents non-oriented substances.

In Fig. 7 the orientation of the polymers in the compound middle lamella region of the spruce wood section is shown. Although the lignin composition differs somewhat in terms of its basic units from that in the S_2 wall, all lignin units have the similar based absorbance peak around 1506 cm^{-1} (Faix 1991). Due to the size of the pixel resolution of

the imaging FTIR of 6.25 μm x 6.25 μm, there is an overlap to the primary, S_1 and S_2 walls. It is here clear that the lignin in the middle lamella region shows a complete lack of orientation (the orientation distribution vector is the same in all directions; the dotted line), i.e. the lignin is isotropic. For the cellulose two different orientations are seen, one at about 90° and one being 0°. It could here be speculated that the 90° oriented component could come from microfibrils in the S_1 layer, while the 0° contribution would come from a part of the S_2 wall being incorporated in the view of the image examined.

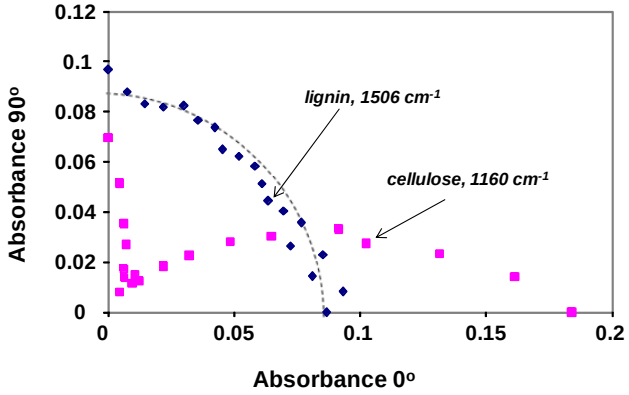

Fig. 7. Polar diagram (0° to 90°) of the absolute absorbance of lignin and cellulose for a middle lamella area of spruce wood. 0° polarization is in the longitudinal fiber direction. Each data point represents a measurement between 0° and 90° polarization taken every 5°. The dotted line represents non-oriented substances.

Serbian Spruce

In Fig. 8 the orientation distribution is illustrated for fibers from a branch of Serbian spruce. Evidently there was here a clear component of the lignin that is oriented more or less in the direction of the fiber axis and the cellulose microfibrils. It is at the same time clear that some parts of the lignin are less organized, displaying a more isotropic behavior.

Hybrid Aspen

The orientation distribution of lignin and cellulose in a hybrid aspen is displayed in Fig. 9. In this case the area examined was composed of both the cell wall areas as well as the middle lamella region connecting the fibers. Although a component of lignin orientation in the direction of the cellulose direction and the fiber direction is visible, it is clear that the isotropic component was much larger than for the other materials examined. This fact could well be based on the fact that the lignin signal was a mix of lignin from a totally isotropic middle lamella region and from the secondary wall region displaying some degree of orientation of the lignin.

Maple

Figure 10 displays the orientation distribution for branch fibers from maple. Also in this case, a large part of the lignin shows an orientation in the direction of the cellulose microfibrils and the fiber axis. Still a considerable part of the lignin must be considered as non-oriented.

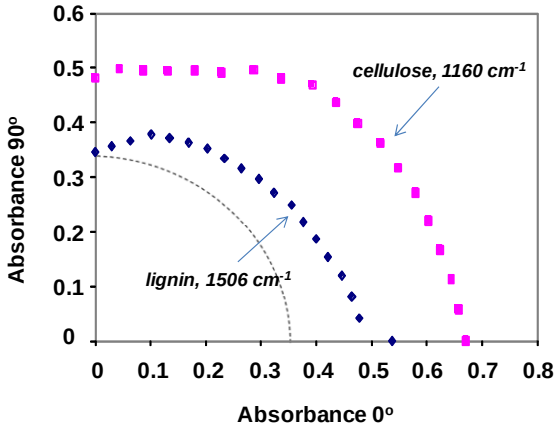

Fig. 8. Polar diagram (0° to 90°) of the absolute absorbance of lignin and cellulose from a branch fiber of Serbian spruce. 0° polarization is in the longitudinal fiber direction. Each data point represents a measurement between 0° and 90° polarization taken every 5°. The dotted line represents non-oriented substances.

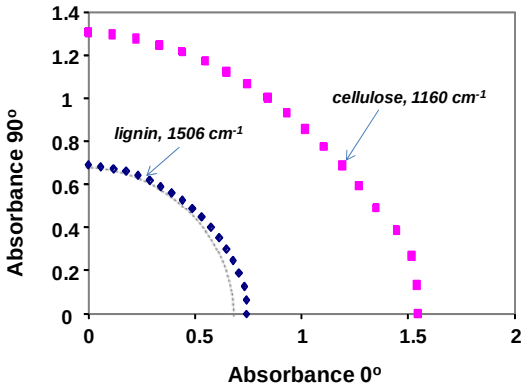

Fig. 9. Polar diagram (0° to 90°) of the absolute absorbance of lignin and cellulose for wood section of middle lamella and fiber walls from a hybrid aspen. 0° polarization is in the longitudinal fiber direction. Each data point represents a measurement between 0° and 90° polarization taken every 5°. The dotted line represents non-oriented substances

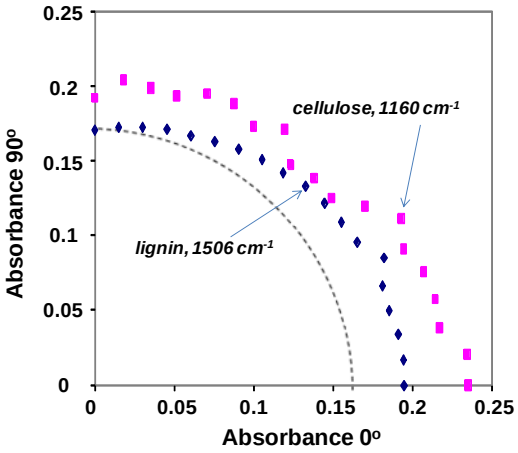

Fig. 10. Polar diagram (0° to 90°) of the absolute absorbance of lignin and cellulose from a branch fiber of maple. 0° polarization is in the longitudinal fiber direction. Each data point represents a measurement between 0° and 90° polarization taken every 5°. The dotted line represents non-oriented substances

Cell Wall Structure

From the results here obtained, it seems clear that some parts of the lignin in the secondary cell wall structure of all fiber types examined show an orientation distribution. This part of the lignin seems to have an orientation in the direction of the cellulose microfibrils and the fiber axis. This may be a reflection of the fact that lignin formation occurs after that the cellulose microfibril/hemicellulose aggregate structure has been formed, serving as the template for the lignin deposition. The cellulose aggregate structure have been shown to possess an undulation structure in the secondary wall, as viewed from electron microscopy (Duchesne and Daniel 1999 ; Bardage et al. 2004), and earlier speculated on (Boyd 1982). This could probably also account for some of the variation in orientation seen for the cellulose component. The undulating structure results in elliptical pores, which are created with an aspect ratio larger than one in the direction

of the cellulose microfibrils, i.e. the pores are longer in the direction of the fiber axis (Bardage et al. 2004); this phenomenon is schematically illustrated in Fig. 11. As compared to the cellulose aggregates of a mean diameter of 16 nm (Bardage et al. 2004 ; Salmén and Fahlén 2006) the elliptical pores have been estimated to have a length to width ratio of about 2 with a width in the range of 5 to 10 nm (Bardage et al. 2004 ; Salmén and Fahlén 2006). Due to the limited size of these pores it is to be expected that when lignin polymerizes in the spaces between the carbohydrate aggregates, an orientation in the longitudinal direction of the pores will be favored due to spatial limitations. Strong non-covalent attractive interactions between the phenyl rings and the OH-groups of the carbohydrates may also be expected to contribute to an orientation in the direction of the cellulose microfibrils. Molecular dynamics modeling have also indicated a structured orientation of lignin model oligomers in parallel to carbohydrate surfaces (Houtman and Atalla 1995).

For the lignin polymerized in the middle lamella region such constraints do not exist, and this explains why a more random structure may be created. The lignin macromolecule is highly flexible, probably due to the large amount of ester bonds, and it can easily assume many different stable or meta-stable conformations, resulting in reversible dramatic changes in molecular size and volume (Micic et al. 2002). Thus the non-oriented structure of the lignin indicted from Fig. 7 seems as a confirmation of such a random lignin structure. The differences in the organization of the two types of lignin should have an impact on both mechanical and chemical properties of the different cell wall structures.

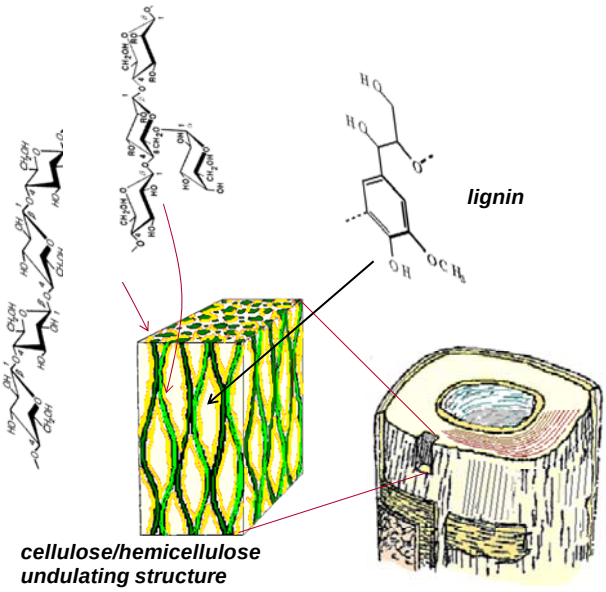

Fig. 11. Schematic structure of the secondary cell wall of a softwood tracheid, diameter ca 35 μm with the undulating cellulose/hemicellulose aggregate structure oriented in the fiber direction. This picture is not to scale for clarity. Cellulose aggregates have an average diameter of 16 nm with the elliptical spaces in-between having a length to with ratio of about 2 and a minor diameter across the ellipse of 5 to 10 nm. These spaces left over after the initial deposition of the cellulose/hemicellulose aggregates will structure the organization of the lignin molecules deposited afterwards.

CONCLUSIONS

1. It is shown that the lignin in both the tree trunk and in its branches, for both hardwood and softwood species, are to some extent structurally ordered with a preferred direc-

tionality following that of the cellulose microfibrils and the longitudinal direction of the fibers.
2. It is believed that this structuring of the lignin in the S_2 layer of the cell wall might be the result of the spatial constrains within the cell wall, as occurring due to the previously deposited cellulose/hemicellulose organization of a strongly oriented assembly.
3. By contrast, it is indicated that the lignin deposited within the middle lamella region displays a totally isotropic, i.e. non-oriented, structure.

ACKNOWLEDGMENTS

This work was funded in part by Biomime, the Swedish Centre for Biomimetic Fibre Engineering (a collaboration between the Schools of Biotechn. and Chem. Sci. and Eng. at KTH, the Umeå Plant Science Centre (UPSC), and Innventia), and in part by the Wallenberg Wood Science Center (WWSC) of KTH and Chalmers. Grant 173017 of the Ministry of Science and Technology of the Republic of Serbia also supported this study.

REFERENCES CITED

Åkerholm, M., Hinterstoisser, B., and Salmén, L. (2004). "Characterization of the crystalline structure of cellulose using static and dynamic FT-IR spectroscopy," *Carbohydr. Res*. 339, 569-578.

Åkerholm, M., and Salmén, L. (2001). "Interactions between wood polymers studied by dynamic FT-IR spectroscopy," *Polymer* 42, 963-969.

Åkerholm, M., and Salmén, L. (2003). "The oriented structure of lignin and its viscoelastic properties studied by static and dynamic FT-IR," *Holzforschung* 57, 459-465.

Atalla, R. H., Hackney, J. M., Uhlin, I., and Thompson, N. S. (1993). "Hemicelluloses as structure regulators in the aggregation of native cellulose," *Int. J. Biol. Macromol.* 15(2), 109-112.

Bardage, S., Donaldson, L., Tokoh, C., and Daniel, G. (2004). "Ultrastructure of the cell wall of unbeaten Norway spruce pulp fibre surfaces," *Nordic Pulp & Paper Research Journal* 19(4), 448-452.

Bergander, A., Brändström, J., Daniel, G., and Salmén, L. (2002). "Fibril angle variability in earlywood of Norway spruce using soft rot cavities and polarization confocal microscopy," *J. Wood Science* 48(4), 255-263.

Bjurhager, I., Olsson, A. M., Zhang, B., Gerber, L., Kumar, M., Berglund, L. A., Burgert, I., Sundberg, B., and Salmén, L. (2010). "Ultrastructure and mechanical properties of *Populus* wood with reduced lignin content caused by transgenic down-regulation of cinnamate 4-hydroxylase," *Biomacromolecules* 11(9), 2359-2365.

Boyd, J. D. (1982). "An anatomical explanation for visco-elastic and mechanosorptive creep in wood, and effects of loading rate on strength," In: *New Perspective in Wood*

Anatomy, Baas, P. (ed.), Martinus Nijhoff/Dr W Junk Publishing, La Hague, pp. 171–222.

Duchesne, I., and Daniel, G. (1999). "The ultrastructure of wood fibre surfaces as shown by a variety of microscopical methods - A review," *Nord. Pulp. Pap. Res. J.* 14(2), 129-139.

Gierlinger, N., Goswami, L., Schmidt, M., Burgert, I., Coutand, C., Rogge, T., and Schwanninger, M. (2008). "In situ FT-IR microscopic study on enzymatic treatment of poplar wood cross-sections," *Biomacromolecules* 9(8), 2194-2201.

Gierlinger, N., Schwanninger, M., Reinecke, A., and Burgert, I. (2006). "Molecular changes during tensile deformation of single wood fibers followed by Raman microscopy," *Biomacromolecules* 7(7), 2077-2081.

Faix, O. (1991). "Classification of lignins from different botanical origins by FTIR spectroscopy," *Holzforschung* 45, 21-27.

Houtman, C. J., and Atalla, R. H. (1995). "Cellulose-lignin interactions: A computational study," *Plant Physiol.* 107(3), 977-984.

Hsieh, Y.-C., Yano, H., Nogi, M., and Eichhorn, S. J. (2008). "An estimation of the Young's modulus of bacterial cellulose filaments," *Cellulose* 15, 507-513.

Jurasek, L. (1998). "Molecular modelling of fibre walls," *J. Pulp Pap. Sci.* 24, 209-212.

Liang, C. Y., and Marchessault, R. H. (1959). "Infrared spectra of crystalline polysaccharides. II. Native celluloses in the region from 640 to 1700 cm^{-1}," *J. Polym. Sci.* 39, 269-278.

Marchessault, R. H. (1962). "Application of infra-red spectroscopy to cellulose and wood polysaccharides," *Pure Appl. Chem.* 5, 107-129.

Micic, M., Orbulescu, J., Radotic, K., Jeremic, M., Sui, G., Zheng, Y., and Leblanc R. M. (2002). "ZL-DHP lignin model compound at the air–water interface," *Biophysical Chemistry* 9, 955-962.

Olsson, A.-M., Bjurhager, I., Gerber, L., Sundberg, B., and Salmén, L. (2011). "Ultra-structural organisation of cell wall polymers in normal and tension wood of aspen revealed by polarisation FT-IR microspectroscopy," *Planta* 233(6), 1277-1286

Page, D. H. (1976). "A note on the cell-wall structure of softwood tracheids," *Wood Fiber* 7, 246-248.

Sahlberg, U., Salmén, L., and Oscarsson, A. (1997). "The fibrillar orientation in the S2-layer of wood fibres as determined by X-ray diffraction analysis," *Wood Sci. Technol.* 31, 77-86.

Salmén, L. (2004). "Micromechanical understanding of the cell wall structure," *C. R. Biologies* 327(9-10), 873-880.

Salmén, L., and Bergström, E. (2009). "Cellulose structural arrangement in relation to spectral changes in tensile loading FTIR," *Cellulose* 16, 975-982.

Salmén, L., and Fahlén, J. (2006). "Reflections on the ultrastructure of softwood fibres." *Cell. Chem. Technol.* 40(3-4), 181-185.

Simonović, J., Stevanic, J., Djikanović, D., Salmén, L., and Radotić, K. (2011). "Anisotropy of cell wall polymers in branches of hardwood and softwood – A polarized FTIR study," *Cellulose*, online DOI 10.1007/s10570-011-9584-1

Stevanic, J., and Salmén, L. (2009). "Orientation of the wood polymers in spruce wood fibres," *Holzforschung* 63, 497-503.

Terashima, N. (1990). "A new mechanism for formation of a structurally ordered protolignin macromolecule in the cell wall of tree xylem," *J. Pulp Pap. Sci.* 16, J150-J155.

Terashima, N., Kitano, K., Kojima, M., Yoshida, M., Yamamoto, H., and Westermark, U. (2009). "Nanostructural assembly of cellulose, hemicellulose, and lignin in the middle layer of secondary wall of ginkgo tracheid," *J. Wood Sci.* 55, 409-416.

Wiley, J. H., and Atalla, R. H. (1987). "Band assignments in the Raman spectra of celluloses," *Carbohydrate Research* 160, 113-129.

Article submitted: August 19, 2011; Peer review completed: September 24, 2011; Revised version received and accepted: November 26, 2011; Published: November 28, 2011.